Probabilistic Multi-Temporal Land Use and Land Cover Change Analysis Using Random Forest and Sentinel-2 Data in Haridwar, India

Shilpa Suman[1*], Abhishek Rawat[1], Anil Kumar[2]
[1]CSE (GIS), NIIT University, Neemrana, Rajasthan, India
[2]PRSD Department, IIRS, Dehradun, Uttarakhand, India
*Corresponding Author email: shilpa.suman011@gmail.com

(Received on 17 March 2026; In final form on 08 October 2026)

DOI: *https://doi.org/10.58825/jog.2026.20.2.320*

Abstract: Multitemporal satellite images are useful for analyzing Land Use Land cover (LULC). It captures temporal images which are used to analyze the gradual transition which are difficult to detect with single date observations. This study focused on detecting the changes in LULC using multi-temporal approach for sentinel-2 images from 2017 to 2025.The approach obtains statistical results and different maps like the hard LULC maps, class wise probability maps, persistence, class to class change detection maps. Random Forest (RF) classifier has been used for classifying the stack of multispectral bands and different indices (Normalized Difference Water Index (NDWI), Normalized Difference Vegetation Index (NDVI), Normalized Difference Built-up Index (NDBI), Modified Normalized Difference Water Index (MNDWI), and Land Surface Water Index (LSWI), Normalized Difference Red Edge Index (NDRE)). Seasonal composites (January-April) were created to assess phenological regularity. Annual classification accuracy was high, ranging from 93.18% to 96.25% with Kappa coefficients of 0.92 to 0.96. Temporal Persistence analysis using a threshold greater than equal to six years to identify the stable classes. Statistics output indicated class specific temporal changes like vegetation phenology, hydrological dynamics, and land management techniques. The results show effectiveness of probabilistic multi-temporal analysis in capturing the gradual LULC changes.

Keywords: Land use/land cover (LULC); Change detection; Random Forest; Multi-temporal analysis; Probabilistic classification; Land cover persistence; GEE.

1. Introduction

Land use and Land cover (LULC) change is an important parameter for environmental changes and human natural interactions. It impacts on ecosystem services, biodiversity, hydrological processes and climate regulation (Lambin et al. 2001). Effective monitoring of LULC changes is crucial for sustainable land management, environmental assessment, and policymaking. Satellite remote sensing is a popular data source for LULC mapping due to its topographical coverage, accuracy, and cost-effectiveness (Lu et al. 2004).

In traditional LULC change detection studies, single-date or bi-temporal classification is commonly used to detect land-cover changes through comparing hard class labels at two time points (Zhu et al. 2024). However, these techniques may not be able to sufficiently capture gradual, seasonal, and annual changes in land cover in dynamic landscapes (Lu and Weng 2007), particularly when land-cover classes have gradual transitions or temporal variability. Especially when distinct classes demonstrate identical spectral responses at a specific time. Multi-temporal satellite data can improve land-cover classification and output stability by capturing temporal data and phenological responses (Pelletier et al. 2016).

The Sentinel-2 satellite data spatial resolution, frequent revisit time, and addition of red-edge and shortwave infrared bands have significantly increased the ability to map LULC (Jocea et al. 2025). Sentinel 2 data have been found to perform well in multi-class LULC classification tasks using machine learning classifiers like RF (Belgiu and Drăguţ 2016; Rodriguez-Galiano et al. 2012). Remote sensing applications utilize Random Forest classifier robustness against noise, ability to handle high-dimensional data, and internal accuracy calculations.

Despite advancements, most multi-temporal LULC research still utilize hard categorized outputs, assuming equal confidence in time and space. Foody (2002) suggests that the lack of systematic assessment of classification ambiguity and inter-annual variance may lead to biased change detection. Random Forest probabilistic classification outputs, such as per-pixel class probabilities, offer an opportunity to incorporate uncertainty into temporal analysis beyond discrete class labels (Zhu and Woodcock 2014).

This paper presents a probabilistic approach for analyzing LULC variation across multiple years, utilizing Sentinel-2 data from 2017-2025. Land-cover stability, persistence, and change are assessed by stacking per-pixel class probability estimates throughout time, in addition to basic pixel-level transitions. A confidence-based persistence rule separates stable and transitional land-cover zones, reducing the influence of seasonal fluctuations and classification errors. The proposed methodology utilizes the RF classifier combines spectral indices sensitive to vegetation, water, and built-up with probabilistic Random Forest classification to provide a robust and uncertainty-aware framework for monitoring LULC over long periods.

© Indian Society of Geomatics

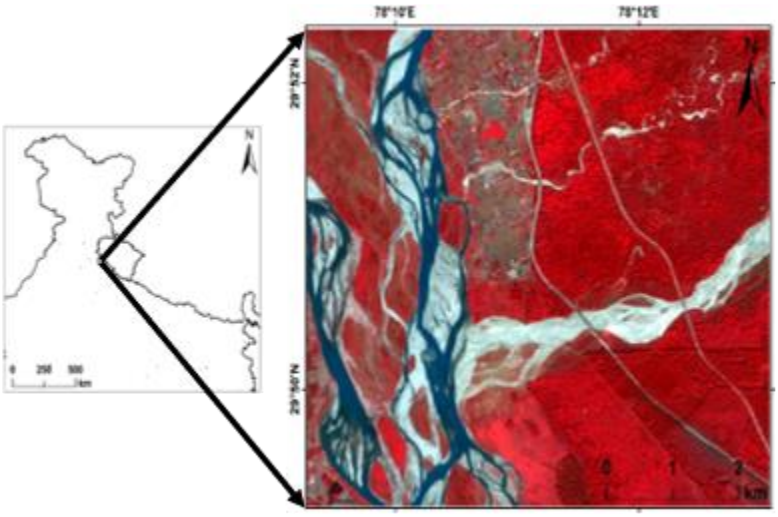


Figure 1: Location map of the study area in Haridwar district, Uttarakhand, India. It shows the boundary of the study region. It is used for multi-temporal LULC classification using Sentinel-2 imagery.

2. Mathematical Concept of classifier and Indices

Section 2 considers the mathematical explanations for different indices and Machine Learning used in this work. The RF Classifier (Pal 2005), NDVI (Suman et al. 2023), NDWI (Gao 1996), MNDWI (Singh et al. 2015), NDBI (Zheng et al. 2021), NDRE (Boiarskii and Hasegawa 2019) and LSWI (Chandrasekar et al. 2010)

2.1 Random Forest Classifier

RF classifiers construct various decision trees using bootstrap samples and randomly selected features. Then it classifies each tree by vote of majority. It is known to be supervised ensemble learning technique which is used in LULC classification. RF accuracy and stability is excellent, and it also reduces overfitting. Eq. 1 describes the calculation of RF.

$$\hat{\boldsymbol{y}}=\text{mode}\ \{\boldsymbol{h_t(x)}\},\ t = 1, 2,\ldots, T \qquad \text{Eq. 1}$$

Where $h_t(x)$ is the prediction of the t^{th} decision tree and T is the total number of trees.

2.2 NDVI

NDVI is very useful and easy for measuring dynamic vegetation changes. NDVI values close to one for dense and diverse vegetation while it shows near to zero for sand and barren soil. This is commonly used in agriculture and environmental studies as a vegetation indicator. Eq. (2) describes the calculation of NDVI.

$$\mathbf{NDVI} = \frac{\mathbf{R_{NIR}-R_{RED}}}{\mathbf{R_{NIR}+R_{RED}}} \qquad \text{Eq. 2}$$

R_{NIR} and R_{RED} represent the reflectance values of the near-infrared and red spectral bands, respectively.

2.3 NDWI

NDWI is the most utilized indices which are used for identifying and monitoring the water content. It calculates the positive value for the water bodies while showing the low or negative for vegetation and soil. It is efficient for finding water in multispectral images. The NDWI is calculated as Eq. (3)

$$\mathbf{NDWI} = \frac{\mathbf{R_{GREEN}-R_{NIR}}}{\mathbf{R_{GREEN}+R_{NIR}}} \qquad \text{Eq. 3}$$

Where R_{GREEN} and R_{NIR} denote the reflectance values of the green and near-infrared bands, respectively.

2.4 MNDWI

MNDWI was introduced to enhance the detection of water bodies in urban and built-up areas. MNDWI indicates positive value for water bodies while it represents negative value for built up areas. The MNDWI is expressed as Eq. (4).

$$\mathbf{MNDWI} = \frac{\mathbf{R_{GREEN}-R_{SWIR}}}{\mathbf{R_{GREEN}+R_{SWIR}}} \qquad \text{Eq. 4}$$

Where R_{GREEN} and R_{SWIR} represent reflectance values of the green and short-wave infrared bands, respectively.

2.5 NDBI

NDBI is used for mapping and detecting the urban/built up land use. NDBI values are higher than vegetation and water surfaces. This index is very useful for showing the urban growth and change land studies. The NDBI is calculated by the Eq. (5).

$$\mathbf{NDBI} = \frac{\mathbf{R_{SWIR}-R_{NIR}}}{\mathbf{R_{SWIR}+R_{NIR}}} \qquad \text{Eq. 5}$$

Where R_{SWIR} and R_{NIR} denote the reflectance values of the short-wave infrared and near-infrared bands, respectively.

2.6 NDRE

NDRE is a vegetation index that is sensitive to chlorophyll content and canopy structure. It is used when the NDVI saturates in dense vegetation. This is useful for monitoring crop health and precision agriculture. NDRE is defined by Eq. (6).

$$\mathbf{NDRE} = \frac{\mathbf{R_{NIR}-R_{RE}}}{\mathbf{R_{NIR}+R_{RE}}} \qquad \text{Eq. 6}$$

Where R_{NIR} and R_{RE} represent reflectance values of the near-infrared and red-edge bands respectively.

2.7 LSWI

LSWI index is used to calculate vegetation and soil moisture content. It utilizes the sensitivity of the short-wave infrared band. Higher value of LSWI indicates higher moisture content, whereas lower value represents dry surface. The LSWI is computed using Eq. (7).

$$\mathbf{LSWI} = \frac{\mathbf{R_{NIR} - R_{SWIR}}}{\mathbf{R_{NIR} + R_{SWIR}}} \qquad \text{Eq. 7}$$

Where R_{NIR} and R_{SWIR} correspond to reflectance values of the near-infrared and short-wave infrared bands respectively.

3. Study Area and Dataset

This research used Sentinel-2 Satellite temporal images. Figure 1 represent the study region, which is in Haridwar district, Uttarakhand, India. Due to heterogeneity LULC makes it ideal for choosing this area and applying the LULC analysis. The research area extends to 5.92 km east-west and 5.95 km north-south, with latitudes 29°49′14″ N to 29°52′21″ N and longitudes 78°09′17″ E to 78°13′04″ E. This region mainly consists of six Classes which are as follows Dense Forest, Eucalyptus, Grassland, Riverine Sand/Build up, Wheat and Water. For Analysis this paper uses multiple periods from 2017 to 2025 to capture medium-term LULC dynamics. This time period is sufficient to detect continuing changes in vegetation, agricultural land, riverine sand, built-up areas, and water bodies (Pelletier et al. 2016). Haridwar district has been chosen because it is a dynamic landscape that includes agricultural fields, forests, riverine ecosystems and rapidly expanding built-up areas. The district has witnessed substantial LULC changes such as urbanisation, expansion of agriculture, and infrastructural development, which makes it an ideal location for conducting spatio-temporal LULC analysis. The chosen agricultural region is representative of these changing landscapes and major land-cover classes including wheat, forests, eucalyptus, grassland, water and river sand. The period of study (2017-2025) was selected to examine recent LULC dynamics with consistent Sentinel-2 images allowing reliable monitoring of landscape changes and facilitating sustainable land management (Singhal et al. 2021; Suman et al. 2022).

4. Methodology Adopted

Figure 2 depicts the technique and process flow used in this research. The major goal of this study is to examine multi-temporal LULC dynamics using Sentinel-2 satellite images and a RF based probabilistic classification methodology. The effect of multi-year temporal information and spectral indices on LULC separability and change detection was investigated over the study region from 2017 to 2025. Multispectral bands and important spectral indices such as NDVI, NDWI, MNDWI, NDBI, NDRE, and LSWI were developed to improve class recognition in varied terrain settings. To preserve phenological stability throughout time, annual seasonal composites were created using Sentinel-2 data collected between January and April. This period was also selected because at this time obtained cloud free Sentinel-2 imagery. In contrast, post-monsoon imagery is often affected by residual cloud cover, variable soil moisture, and temporary flooding, which may increase spectral variability and reduce classification consistency across years.

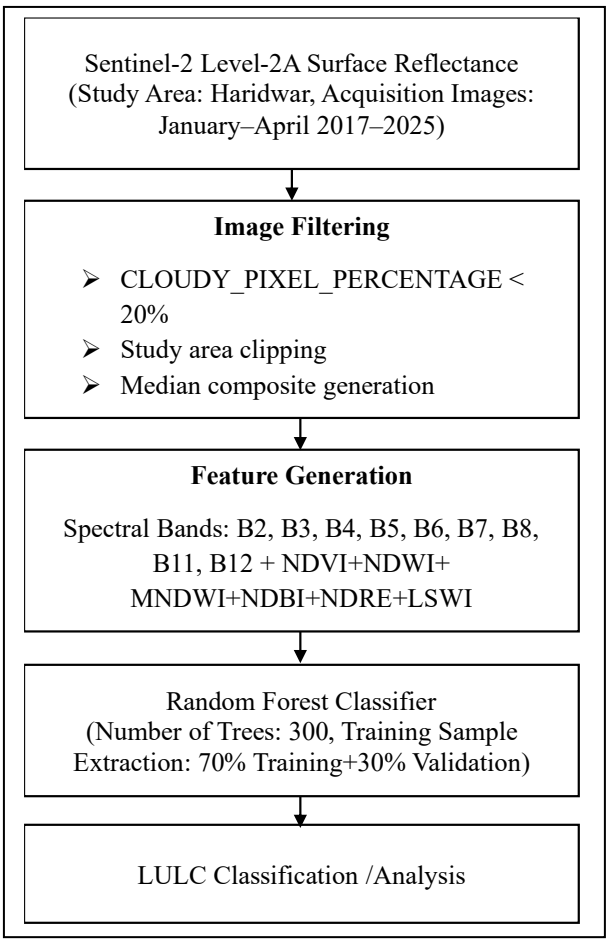


Figure 2: Methodology Workflow

The RF classifier was used to generate yearly LULC maps and per-pixel class probability estimations. These probability outputs were then stacked temporally to evaluate land cover stability, persistence, and transition behavior during the study period. To identify unaffected locations, class-wise stability and persistence maps were created, whereas probabilistic change detection maps were used to quantify gradual and abrupt land cover shifts. The general process was carried out using the Google Earth Engine (GEE) cloud computing environment, and the methodological steps are described below.

Step 1: Sentinel-2 Level-2A Surface Reflectance (SR) imagery was downloaded from Google Earth Engine (GEE) for each year of the study from 2017 to 2025. Images acquired between January and April were considered as the season of interest. Images with less than 10% cloud cover were selected to reduce the effects of cloud contamination. Cloud and cirrus contaminated pixels were masked using the QA60 quality assurance band. The Sentinel-2 Level-2A product is already geometrically co-registered and atmospherically corrected to surface reflectance, therefore no further atmospheric correction or image registration was applied.

Step 2: All rectified Sentinel-2 observations acquired in January to April of each year was merged after

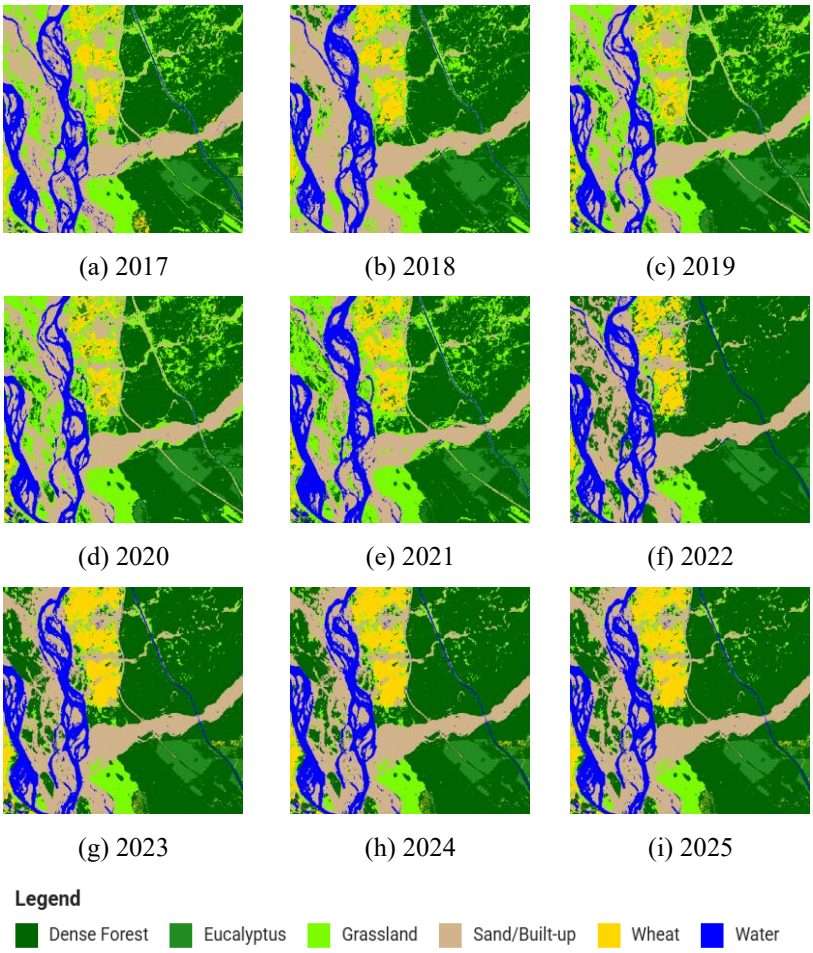


Figure 3 (a-j): Annual Land Use/Land Cover Maps (2017–2025) Derived from Sentinel-2 Imagery Using Random Forest Classification

preprocessing to create one seasonal median composite per year, resulting in annual composites for 2017–2025. To minimize the effects of residual clouds, shadows, atmospheric variability and other anomalous observations, the median operation was applied pixel by pixel. Then, NDVI, NDWI, MNDWI, NDBI, NDRE and LSWI were calculated using the equations described in Section 2.3 based on the annual seasonal composites. Derived spectral indices were incorporated to improve the spectral separability of the different land-cover classes.

Step 3: The generated spectral bands and indices database was classified by the RF classifier to produce per-pixel class probability outputs and annual LULC maps. The training labels were derived from a manually prepared ground-truth dataset consisting of 100 representative samples for each of the six LULC classes. The labelled samples were imported into Google Earth Engine and randomly divided into 70% and 30% training and validation datasets for Random Forest classification.

Step 4: Stack the yearly class probability outputs to examine seasonal probability changes for each land cover class.

Step 5: Create class-specific stability and persistence maps by finding pixels with low probability variations during the period.

Step 6: Generate probabilistic change detection and transition maps to identify both slow and sudden land use changes.

The Random Forest classifier was trained using Sentinel-2 surface reflectance bands (B3, B4, B5, B8 and B11) along with NDVI, NDWI, MNDWI, NDBI, NDRE and LSWI. These variables were chosen because they are good indicators of the vegetation, water bodies, built-up areas and moisture conditions, thus improving the class separability. The number of trees was set to ensure stable classification with little overfitting as recommended by Pal in 2005 (Pal 2005).

A confusion matrix was employed to evaluate the classification accuracy on an independent validation dataset. Overall Accuracy (OA), Producer's Accuracy (PA), User's Accuracy (UA) and the Kappa coefficient were calculated for each annual LULC map. These metrics were used to assess classification reliability and class-wise performance prior to temporal analysis.

5. Results and Discussions

This Result and Discussion part has been divided into four experiments. First Experiment obtain the Hard Classification by Random Forest Classifier and calculating the Overall Accuracy. Second Experiment calculates the probability-based classes and statistical analysis. Third Experiment Shown the Stable and persistence map and last experiment show the change detection in the study region.

Table 1: PA, UA, Overall Accuracy and Kappa value of Random Forest Based LULC Classification from 2017 to 2019

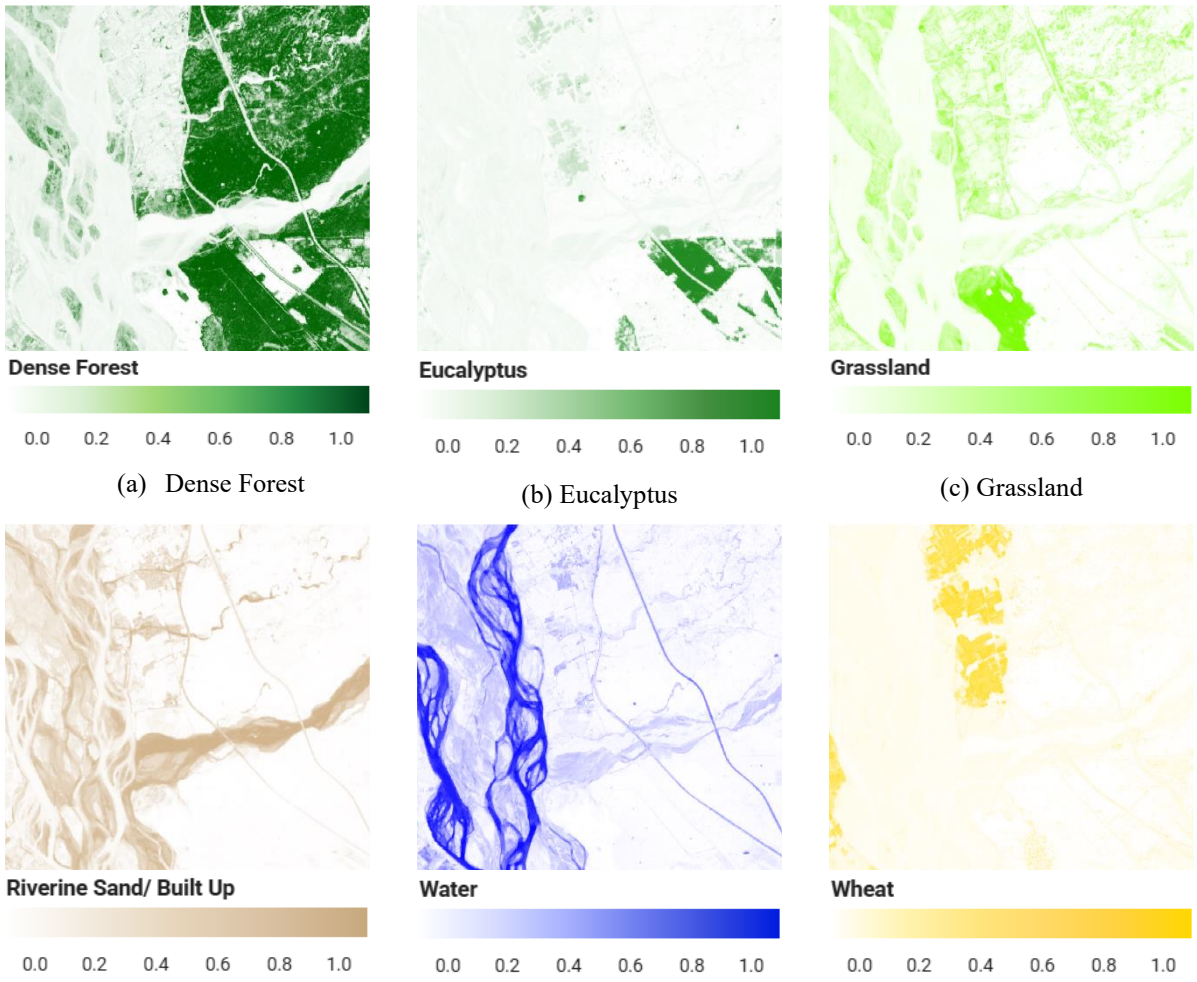
	2017			2018			2019		
	PA	**UA**	**Kappa**	**PA**	**UA**	**Kappa**	**PA**	**UA**	**Kappa**
Dense Forest	96.67	100	0.98	100	100	1	96.67	100	0.98
Eucalyptus	100	100	1	100	100	1	100	100	1
Grassland	100	100	1	100	100	1	100	100	1
Wheat	100	96.29	0.98	100	100	1	100	96.29	0.98
Water	75.00	84.10	0.76	96.43	81.82	0.8609	78.57	84.61	0.78
Sand/Buit-up	96.67	100	0.98	82.35	96.55	0.8643	86.67	81.25	0.80
Overall Accuracy		93.29			95.66			93.60	
Kappa		0.92			0.95			0.92	

Table 2: PA, UA, Overall Accuracy and Kappa value of Random Forest Based LULC Classification from 2020 to 2022

	2020			2021			2022		
	PA	**UA**	**Kappa**	**PA**	**UA**	**Kappa**	**PA**	**UA**	**Kappa**
Dense Forest	96.67	96.67	0.96	100	100	1	100	96.67	0.98
Eucalyptus	96.30	100	0.98	100	100	1	96.43	100	0.98
Grassland	100	100	1	100	100	1	100	100	1
Wheat	100	96.30	0.98	100	100	1	100	100	1
Water	75.00	84.00	0.76	92.86	81.25	0.8388	91.89	94.44	0.92
Sand/Buit-up	86.67	78.79	0.79	82.35	93.33	0.8468	94.44	91.89	0.92
Overall Accuracy		93.18			95.38			96.01	
Kappa		0.92			0.94			0.95	

Table 3: PA, UA, Overall Accuracy and Kappa value of Random Forest Based LULC Classification from 2023 to 2025

	2023			2024			2025		
	PA	**UA**	**Kappa**	**PA**	**UA**	**Kappa**	**PA**	**UA**	**Kappa**
Dense Forest	100	100	1	100	96.67	0.98	100	100	1
Eucalyptus	100	100	1	96.43	100	0.98	100	100	1
Grassland	100	100	1	100	100	1	100	100	1
Wheat	100	100	1	100	100	1	100	100	1
Water	96.43	84.38	0.8788	91.89	91.89	0.90	78.95	71.43	0.72
Sand/Buit-up	84.38	96.43	0.8788	91.67	91.67	0.89	80.65	86.21	0.80
Overall Accuracy		95.88			96.25			94.31	
Kappa		0.96			0.95			0.92	



(a) Dense Forest (b) Eucalyptus (c) Grassland

(d) Riverine Sand/ Built Up (e) Water (f) Wheat

Figure 4 (a-f): Mean Class Probability Maps Derived from Multi-Temporal Random Forest Classification

5.1 Experiment 1: Multi-Temporal LULC Classification Accuracy Assessment Using Random Forest

In Experiment 1, the RF classifier was evaluated on Sentinel-2 data from 2017 to 2025 to generate annual hard LULC maps. Figure 3 presents the annual LULC maps, while Table 2 reports the corresponding Overall Accuracy and Kappa values. The high Overall Accuracy and Kappa coefficients confirm the reliability of the classification for multi-temporal analysis. Limited misclassification is observed in a few transitional areas, particularly along riverine zones.

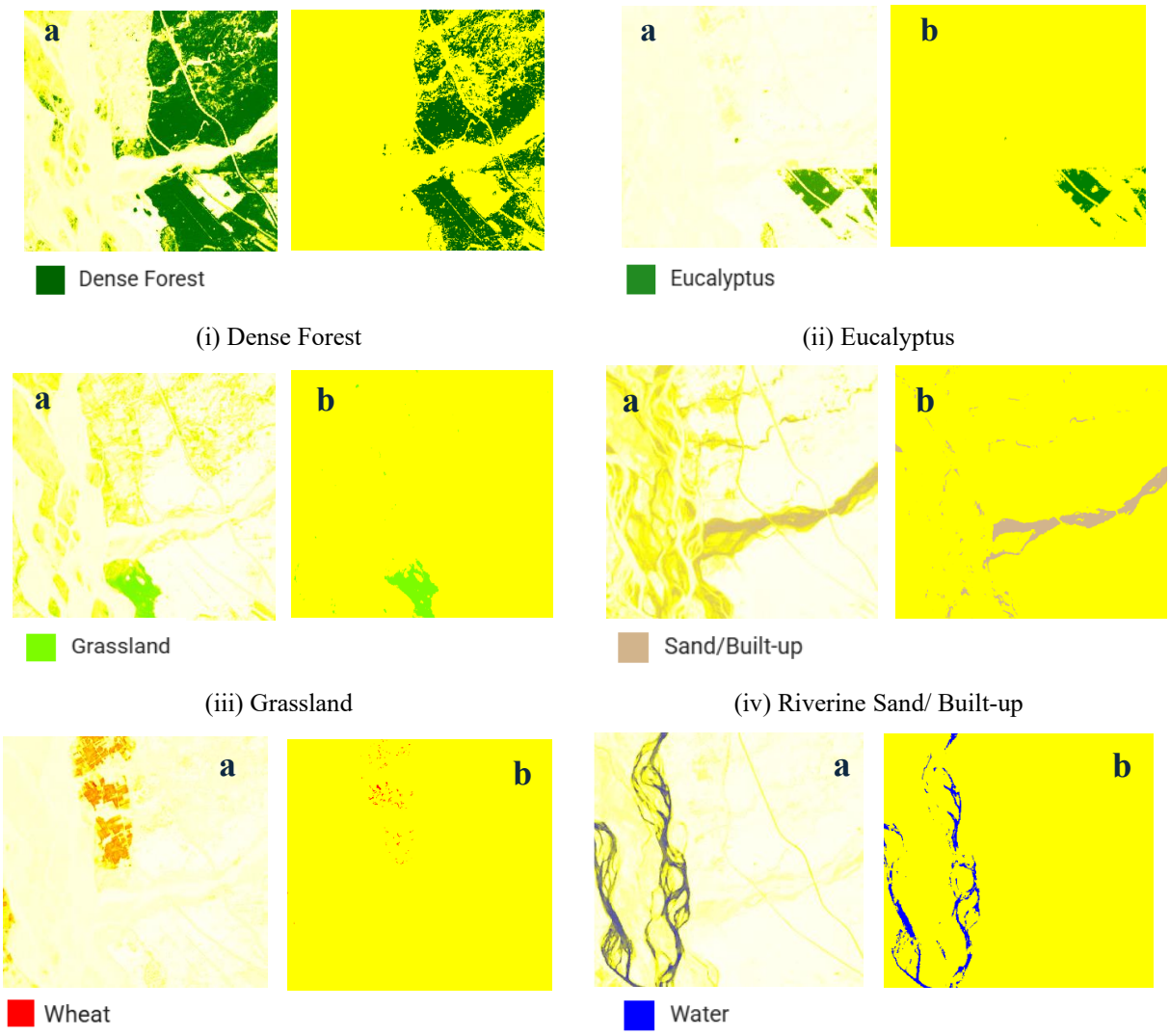
The annual LULC maps indicate largely stable land cover conditions at the landscape level, with no significant abrupt changes observed during the study period. However, the next section shows the class-wise probability mean map (Figure 4). It shows the specific defined six class. This reduces the problem like detecting the small changes occurring by the hard classification. Table 1-3 shows the class-wise assessment. This indicates that Dense Forest, Eucalyptus, Grassland and wheat provide the high Producer's Accuracy (PA) and User's Accuracy (UA). This result indicates that the good class separability. On the other hand, Water and Sand/Buildup were observed less accuracy compared to other classes. The main misclassification occurred along bank of river and flood plain boundaries. Basically, this area's effects are due to seasonal changes, exposed riverine sand and mixed pixels which provide similar spectral responses. Despite this the Overall Accuracy ranging from 93.18% to 96.25% and Kappa coefficients between 0.92 and 0.96. It indicates strong agreement between the classified maps and the reference data.

Accuracy values are changing across years due to Different Factor. The factors are such as image quality, phenological environments, and land heterogeneity. This all-factor impacts spectral separability (Verbesselt et al. 2010).

5.2 Experiment 2: Probability-Based Statistical Characterization of Multi-Temporal LULC Classes

Experiment 2 provided probability-based results (Figure 4) from multi-temporal Random Forest classification was employed to quantitatively describe (Table 2) LULC classes during the study period.

Figure 4 depicts the mean probability maps of all land use/land cover classes derived from multi-temporal classification methodology. Unlike hard classification maps, which each pixel is assigned to a class and are susceptible to spectral confusion, the probability means maps can be used to quantify class membership confidence throughout time. In particular, categories like sand and



(i) Dense Forest (ii) Eucalyptus

(iii) Grassland (iv) Riverine Sand/ Built-up

(v) Wheat (vi) Water

Figure 5 (i-vi): Land Cover Persistence and Stable Area (a) and (b) respectively of LULC

water. Observed changes between Water and Riverine Sand are mainly due to seasonal hydrological variability, such as changes in river discharge, sediment deposition, and exposure of sand bars during flood and dry-season conditions, rather than spectral confusion between these classes. The probabilistic nature of the representation diminishes boundary uncertainties and clustering of misclassification by focusing on stable high class membership probabilities rather than one-date spectral signatures. This enhancement demonstrates the capacity of probability mean mapping to model stable class behavior and reduce transient or mixed-pixels effects in order to perform a more confident spatial representation of complex and spectrally overlapped land cover types.

Table 4 displays the region coverage and probability-based statistical metrics for the discovered LULC classes. Dense Forest (10.78 km²) is the largest class, with a high mean PD value (0.79) and low standard deviation of pixels (0.074), indicating accurate classification with strong confidence throughout seasons. Eucalyptus plantations and grassland are found in smaller areas (0.99 km² and 0.86 km², respectively), with mean probability values exceeding 0.79 for both. Grassland has a wide range of probabilities (0.26) and standard deviations (0.083), likely due to seasonal and phenological variations. Sand and water classes have lower mean probability (0.71 and 0.68 respectively) and wider variation, with sand having a wide range of probability (0.42) and standard deviation (0.136). This variability could be due to spectrum value mixing with the soil and moisture conditions due to seasonal changes. For wheat class the mean value is 0.66 while the standard deviation is 0.164. This variability was obtained due to the cropping cycles and phenological stages in the study period.

5.3 Experiment 3: Temporal Stability and Persistence Analysis of LULC Classes

Experiment 3 assesses temporal persistence and stability using nine annual LULC maps (2017–2025). Persistence indicates the number of years (0–9) a pixel remained in the same LULC class, while stability is determined by applying a persistence threshold of greater than 6 years to identify long-term stable pixels (Zhang et al. 2024). Figure (5)(a) shows the pixel-wise persistence map (0–9 years) for respective classes, whereas Figure (5)(b) presents the stable land-cover area by class based on the greater than 6-year threshold. Dense forest exhibits the highest stability,

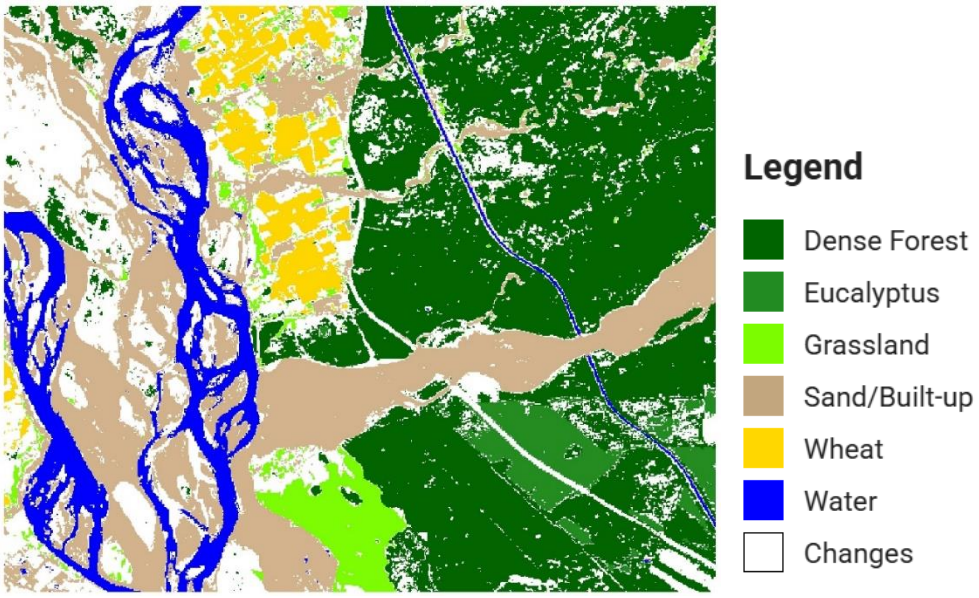


Figure 6: Stable and Transition Classes in the Change Detection Map

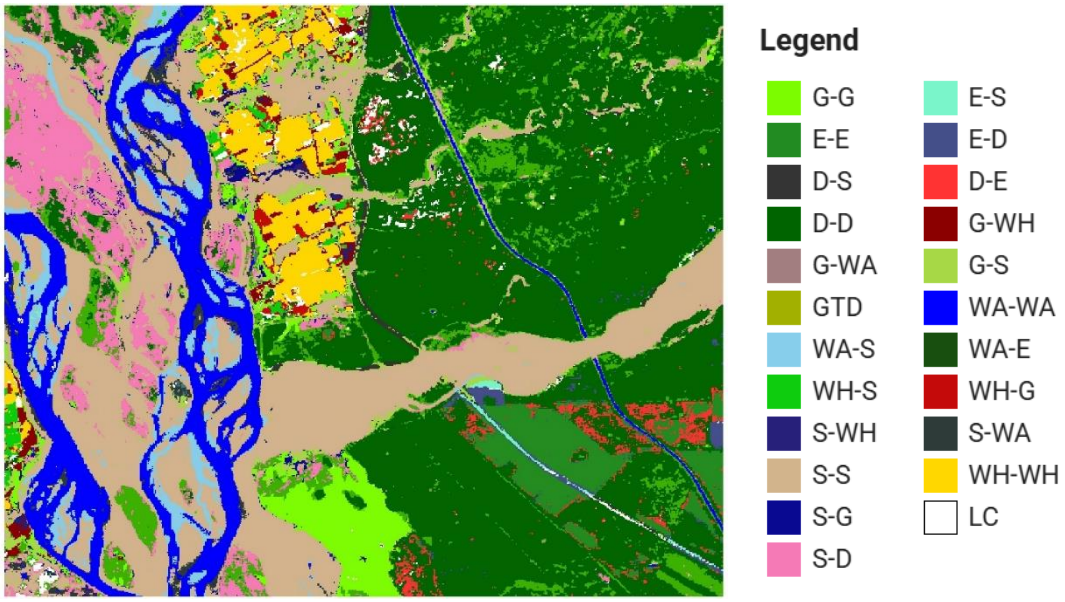


Figure 7: Land Use/Land Cover Change Map Showing Class-to-Class Transitions (2017–2025)

while agricultural and water classes show limited but distinct stable extents.

Table 5 displays the calculated stable areas for each class. Land cover classes showed significant differences in time stability analysis using pixel-wise persistence over nine yearly LULC maps (2017-2025). Land cover pixels were considered stable if they remained in the same class for at least six out of nine years (approximately 70% temporal persistence). This threshold is commonly used in multi-temporal stability studies to account for inter-annual variability and classification uncertainty (Zhang and Roy 2017). The dense forest has the most stable area (7.72 km^2), with minimal disturbance and minor long-term ecological separation. Eucalyptus (0.76 km^2) and grass land shows moderate stability. For Moderate Stability there are different reasons like seasonal variations, vegetation cycles, and human activity. Sand (1.38 Km^2) opposes geomorphic features like riverbanks and active floodplains. Water bodies have a least surface area (0.85 km^2), and it changes highly in season period. Wheat (0.25 km^2) has least area Due to seasonal crops and a rotation cycle.

5.4 Experiment 4: Land Use/Land Cover Transition Analysis (2017–2025)

Experiment 4 shows the LULC transition (change Detection) from 2017-2025. Figures 6 and 7 display the changes between one class to another (from 2017 to 2025). Figure 6 shows the stable class with different colors but changes between one class to another represent by white color. Figure 7 provides the legend, mainly it is used to show the specific transition between the class. In legend D, E, G, S, WH and WT stands for Dense Forest, Eucalyptus, Grassland, Riverine sand/ Buildup, Wheat and Water respectively. There are also some minor changes between one class to another which are represented by the legend LC. The identified LULC transitions were studied carefully by using Sentinel-2 false colour composites, high

Table 4: Area Coverage and Probability-Based Statistical Metrics of LULC Classes

Class	Area km^2	Mean value	Pixel Count	Range Probability	Standard Derivation
Dense Forest	10.77663	0.786983251	124669.7	0.226464	0.074061
Eucalyptus	0.989578	0.810029	11446.35	0.209817	0.068695
Grassland	0.858069	0.79361	9924.784	0.257835	0.083145
Sand/ Built up	2.121867	0.71063	24545.67	0.421752	0.13625
Water	1.564701	0.682681	18100.25	0.295875	0.094978
Wheat	0.896831	0.661286	10376.17	0.496265	0.16394

resolution Google Earth imagery and local knowledge of the study area. Transitions from grassland to dense forest are locally possible and may be investigative of natural vegetation regeneration or increasing canopy density. Wheat to Grassland may also be caused by changes in agricultural practices, fallow periods or abandonment of cultivated fields. On the other hand, transitions like Grassland to Water, Riverine Sand/Built-up to Dense Forest, Riverine Sand/Built-up to Grassland, Eucalyptus to Riverine Sand/Built-up, Eucalyptus to Dense Forest, Dense Forest to Wheat and Water to Eucalyptus are not generally expected during the study period. These transitions only cover a very small proportion of the total area and are thus interpreted as localised classification uncertainty due to mixed pixels, boundary effects, seasonal spectral variability or geolocation differences rather than true land cover conversion. Therefore, the interpretation of the LULC dynamics is mostly based on the dominant and ecologically plausible transitions.

Table 6 shows the stability of land use and changes between 2017 to 2025 for each class. From table it is observed that almost all classes change to Dense Forest. Dense forest has the highest persistence at 92.90% and Grassland has the lowest persistence 27.16% due to restoration or seasonal impact. Percentages represent the proportion of the 2017 source class area transitioning into each different class by 2025. Values for each source class sum to 100%.

Table 5: Stable Area Estimation of LULC Classes Based on Pixel-Wise Temporal Persistence (2017–2025)

Class	Stable Area(km^2)
Dense Forest	7.718
Eucalyptus	0.762
Grassland	0.728
Sand/Built up	1.385
Water	0.854
Wheat	0.246

Most of the land-cover classes were highly persistent between 2017 and 2025 (see Table 6) with a small percentage of pixels changing their classes. The major transitions, namely Grassland to Dense Forest, Dense Forest to Eucalyptus, Wheat to Riverine Sand/Built-up, and Water to Riverine Sand/Built-up, agree with the vegetation succession, plantation development, agricultural practices, and river dynamics in the study area. However, transitions with very small areas (near 0%) such as Water to Dense Forest, Eucalyptus to Water, and Grassland to Water are not considered practically significant. These isolated changes are likely due to mixed pixels, boundary effects, seasonal spectral variability or classification uncertainty rather than actual land-cover conversion. Thus, the analysis of LULC dynamics is focused on common transitions with a considerable spatial extent, considering minor transitions as non-representative of landscape change.

6. Conclusion

This study offers a framework for a probabilistic multi-temporal LULC analysis using Sentinel-2 imagery and the RF classifier to identify land use and land cover changes from 2017 to 2025. The proposed approach integrates class membership probabilities from different years, leading to a more consistent representation of temporal LULC patterns and allowing the detection of persistent land-cover changes. Probability based analysis provides better results compared to hard classification outputs. It detects gradual changes that hard classification is not capable. Pixel-wise temporal persistence analysis was applied to recognize stable land cover variations from temporary or seasonal changes. The output highlights that Dense Forest has high stability compared to other classes. In contrast, grassland, riverine sand/build-up areas, and water bodies exhibit greater temporal variability. These classes

Table 6: Class-to-Class LULC Transition Between 2017 and 2025

From	To	Area km^2	Area Percentage
Dense Forest	Dense Forest	12.632	92.902
	Eucalyptus	0.431	3.171
	Grassland	0.123	0.902
	Riverine Sand/Build up	0.231	1.697
	Wheat	0.174	1.281
	Water	0.006	0.047
Eucalyptus	Eucalyptus	1.068	81.186
	Dense Forest	0.175	13.262
	Grassland	0.003	0.217
	Riverine Sand/Build up	0.057	4.304
	Wheat	0.007	0.529
	Water	0.007	0.502
Grassland	Grassland	1.246	27.156
	Dense Forest	2.161	47.117
	Eucalyptus	0.014	0.315
	Riverine Sand/Build up	0.767	16.726
	Wheat	0.381	8.301
	Water	0.018	0.386
Riverine Sand/Build up	Riverine Sand/Build up	7.518	75.149
	Dense Forest	1.856	18.555
	Eucalyptus	0.015	0.149
	Grassland	0.185	1.844
	Wheat	0.053	0.527
	Water	0.378	3.776
Wheat	Wheat	1.377	80.255
	Dense Forest	0.021	1.206
	Eucalyptus	0.015	0.872
	Grassland	0.141	8.240
	Riverine Sand/Build up	0.161	9.397
	Water	0.000	0.030
Water	Water	2.816	73.071
	Dense Forest	0.006	0.148
	Eucalyptus	0.002	0.054
	Grassland	0.000	0
	Riverine Sand/Build up	1.030	26.725
	Wheat	0.000	0.002

represent more dynamic components. The class-to-class transition analysis shows the changes between the different classes. These changes are due to ecological edges, agricultural boundaries, and river corridors. Changes between water and riverine sand or built-up areas represent hydrological variability. In this study first obtain the probability-based classification it improves the LULC reliability. Second obtain the stability and transition map it

shows the long-term land cover behavior and exposes dynamic class behavior, respectively. Stability and transition maps provide a long-term monitoring framework which enhances the understanding of land cover change processes. Lastly shows the change Detection map which reveals the changes from one class to another between 2017 to 2025. This study helps to monitor the environment, land management, and policy-oriented decision support.

References

Belgiu, M., and L. Drăguţ. 2016. "Random Forest in Remote Sensing: A Review of Applications and Future Directions." *ISPRS Journal of Photogrammetry and Remote Sensing* 114:24–31. https://doi.org/10.1016/j.isprsjprs.2016.01.011

Boiarskii, B., and H. Hasegawa. 2019. "Comparison of NDVI and NDRE Indices to Detect Differences in Vegetation and Chlorophyll Content." *Journal of Mechanics of Continua and Mathematical Sciences* 4:20–29. https://doi.org/10.26782/jmcms.spl.4/2019.11.00003

Chandrasekar, K., M. V. Sesha Sai, P. S. Roy, and R. S. Dwevedi. 2010. "Land Surface Water Index (LSWI) Response to Rainfall and NDVI Using the MODIS Vegetation Index Product." *International Journal of Remote Sensing* 31(15):3987–4005. https://doi.org/10.1080/01431160802575653

Foody, G. M. 2002. "Status of Land Cover Classification Accuracy Assessment." *Remote Sensing of Environment* 80(1):185–201. https://doi.org/10.1016/S0034-4257(01)00295-4

Gao, B. C. 1996. "NDWI—A Normalized Difference Water Index for Remote Sensing of Vegetation Liquid Water from Space." *Remote Sensing of Environment* 58(3):257–266. https://doi.org/10.1016/S0034-4257(96)00067-3

Jocea, A. F., P. Liviu, N. Lucian, and R. Dan. 2025. "Sentinel-2 Land Cover Classification: State-of-the-Art Methods and the Reality of Operational Deployment—A Systematic Review." *Sustainability* 17(22):10324. https://doi.org/10.3390/su172210324

Lu, D., and Q. Weng. 2007. "A Survey of Image Classification Methods and Techniques for Improving Classification Performance." *International Journal of Remote Sensing* 28(5):823–870. https://doi.org/10.1080/01431160600746456

Lu, D., P. Mausel, E. Brondizio, and E. Moran. 2004. "Change Detection Techniques." *International Journal of Remote Sensing* 25(12):2365–2401. https://doi.org/10.1080/0143116031000139863

Lambin, E. F., B. L. Turner, H. J. Geist, S. B. Agbola, A. Angelsen, J. W. Bruce, O. T. Coomes, R. Dirzo, G. Fischer, and C. Folke. 2001. "The Causes of Land-Use and Land-Cover Change: Moving Beyond the Myths." *Global Environmental Change* 11(4):261–269. https://doi.org/10.1016/S0959-3780(01)00007-3

Pal, M. 2005. "Random Forest Classifier for Remote Sensing Classification." *International Journal of Remote Sensing* 26(1):217–222. https://doi.org/10.1080/01431160412331269698

Pelletier, C., S. Valero, J. Inglada, N. Champion, and G. Dedieu. 2016. "Assessing the Robustness of Random Forests to Map Land Cover with High Resolution Satellite Image Time Series over Large Areas." *Remote Sensing of Environment* 187:156–168. https://doi.org/10.1016/j.rse.2016.10.010

Rodriguez-Galiano, V. F., B. Ghimire, J. Rogan, M. Chica-Olmo, and J. P. Rigol-Sanchez. 2012. "An Assessment of the Effectiveness of a Random Forest Classifier for Land-Cover Classification." *ISPRS Journal of Photogrammetry and Remote Sensing* 67:93–104. https://doi.org/10.1016/j.isprsjprs.2011.11.002

Singh, K. V., R. Setia, S. Sahoo, A. Prasad, and B. Pateriya. 2015. "Evaluation of NDWI and MNDWI for Assessment of Waterlogging by Integrating Digital Elevation Model and Groundwater Level." *Geocarto International* 30(6):650–661. https://doi.org/10.1080/10106049.2014.965757

Singhal, M., A. Payal, and A. Kumar. 2021. "Importance of Individual Sample of Training Data in Modified Possibilistic C-Means Classifier for Handling Heterogeneity within a Specific Crop." *Journal of Applied Remote Sensing* 15(3):034507. https://doi.org/10.1117/1.JRS.15.034507

Suman, S., P. K. Pal, A. Kumar, A. Rawat, and A. Singh. 2023. "Convolutional Fuzzy Machine Learning Based Algorithms for Mapping Chickpea Agricultural Crop Fields Using Temporal Satellite Data." *Procedia Computer Science* 230:532–541. https://doi.org/10.1016/j.procs.2023.12.109

Suman, S., D. Kumar, and A. Kumar. 2022. "Fuzzy Based Convolutional Noise Clustering Classifier to Handle the Noise and Heterogeneity in Image Classification." *Mathematics* 10(21):4056. https://doi.org/10.3390/math10214056

Verbesselt, J., R. Hyndman, G. Newnham, and D. Culvenor. 2010. "Detecting Trend and Seasonal Changes in Satellite Image Time Series." *Remote Sensing of Environment* 114(1):106–115. https://doi.org/10.1016/j.rse.2009.08.014

Zhang, H. K., and D. P. Roy. 2017. "Using the 500 m MODIS Land Cover Product to Derive a Consistent Continental Scale 30 m Landsat Land Cover Classification." *Remote Sensing of Environment* 197:15–34. https://doi.org/10.1016/j.rse.2017.05.024

Zhang, X., T. Zhao, H. Xu, W. Liu, J. Wang, X. Chen, and L. Liu. 2024. "GLC_FCS30D: The First Global 30 m Land-Cover Dynamics Monitoring Product with a Fine Classification System for the Period from 1985 to 2022 Generated Using Dense-Time-Series Landsat Imagery and the Continuous Change-Detection Method." *Earth System Science Data* 16(3):1353–1381. https://doi.org/10.5194/essd-16-1353-2024

Zheng, Y., L. Tang, and H. Wang. 2021. "An Improved Approach for Monitoring Urban Built-Up Areas by Combining NPP-VIIRS Nighttime Light, NDVI, NDWI,

and NDBI." *Journal of Cleaner Production* 328:129488. https://doi.org/10.1016/j.jclepro.2021.129488

Zhu, Q., X. Guo, Z. Li, and D. Li. 2024. "A Review of Multi-Class Change Detection for Satellite Remote Sensing Imagery." *Geo-Spatial Information Science* 27(1):1–5. https://doi.org/10.1080/10095020.2022.2128902

Zhu, Z., and C. E. Woodcock. 2014. "Continuous Change Detection and Classification of Land Cover Using All Available Landsat Data." *Remote Sensing of Environment* 144:152–171. https://doi.org/10.1016/j.rse.2014.01.011

.